

# Constant-Time HQQC Experiment for Protein NMR Spectroscopy\*

GRAEME L. SHAW,<sup>†</sup> THOMAS MÜLLER,<sup>‡</sup> HELEN R. MOTT,<sup>†</sup> § HARTMUT OSCHKINAT,<sup>‡</sup>  
IAIN D. CAMPBELL,<sup>†</sup> AND LORENZ MITSCHANG<sup>¶||</sup>

<sup>†</sup>Department of Biochemistry, NMR Protein Structure Group, South Parks Road, Oxford OX1 3QU, United Kingdom;

<sup>‡</sup>Forschungsinstitut für Molekulare Pharmakologie, Alfred-Kowalke-Strasse 4, 10315 Berlin-Friedrichsfelde, Germany;  
and <sup>¶</sup>EMBL, Meyerhofstrasse 1, Postfach 10 2209, D-69012 Heidelberg, Germany

Received September 16, 1996; revised November 12, 1996

One of the most challenging problems for the NMR structure determination of helical proteins is the tendency for the protein core to be made up of aliphatic side chains. The assignment of NOEs between the methyl groups of side chains such as leucine, isoleucine, and valine is often crucial for the precise determination of interhelical angles and the orientation of side chains packed in the core (1–3). The proton chemical shifts of methyl groups are not well dispersed, and it is usually necessary to use <sup>13</sup>C labeling and 3D <sup>13</sup>C-edited NOESY spectra to assign these NOEs (4). The resolution in all three dimensions of these spectra must be as high as possible to resolve the methyl–methyl NOEs, and although a reduced <sup>13</sup>C spectral width improves the resolution in this dimension, one of the <sup>1</sup>H dimensions is usually poorly resolved. The low resolution in the indirect <sup>1</sup>H dimension, combined with the potential overlap of nonmethyl resonances in the <sup>13</sup>C dimension, make the assignment of the methyl–methyl NOEs a problem.

One protein whose spectra have particularly poorly resolved methyl resonances is interleukin 2 (IL-2) (5, 6). IL-2 is a member of the four-helix bundle family of cytokines and plays a crucial role in the immune response. A mutant of IL-2 used in these studies contains 21 Leu, 4 Val, 9 Ile, and 14 Thr residues which could give rise to a total of 82 methyl groups which are expected to resonate within 10 ppm in the <sup>13</sup>C dimension and 0.75 ppm in the <sup>1</sup>H dimension. The majority of these methyl groups are packed together in the hydrophobic core of the protein with relatively few aromatic side chains to disperse their chemical shifts. Three-dimensional <sup>13</sup>C NOESY–HSQC spectra were useful for assigning NOEs between methyl groups in the IL-2 core, but the resolution in this spectrum was still not sufficient to

distinguish all the cross peaks of interest. There are two reasons for the lack of resolution in these spectra: the resolution is limited due to the small number of data points that can be acquired within the available experiment time, and <sup>13</sup>C–<sup>13</sup>C couplings are present in the <sup>13</sup>C dimension. One solution to both of these problems is the use of a HQQC-filtered 3D experiment (7) such as HQQC–NOESY.

The original HQQC (8, 9) experiment uses a DEPT (10)-type transfer to generate heteronuclear quadruple-quantum coherence, which is allowed to evolve under the carbon chemical shifts before being transferred back to the protons where the magnetization is detected; the pulse sequence is shown in Fig. 1a. The phase cycle selects heteronuclear quadruple-quantum coherence during the evolution time, *t*<sub>1</sub>, ensuring only methyl groups are present in the final spectrum. This allows the use of narrow spectral widths in both the proton and carbon dimensions, enabling the acquisition of high-resolution spectra in a reasonable time. However, for uniformly labeled proteins, the resolution in the carbon dimension is reduced due to the presence of unresolved splittings caused by the evolution of the <sup>13</sup>C–<sup>13</sup>C couplings. Thus, the resolution of the HQQC experiment could be improved by removing the modulation due to these couplings, using the constant-time approach (11, 12).

The simplest way to improve the resolution in the carbon dimension is to monitor the <sup>13</sup>C chemical shift during a constant time delay. Figure 1b shows a simple constant-time HQQC experiment in which the *t*<sub>1</sub> evolution time of the HQQC experiment has been made into a constant-time period. The intensity at the start of acquisition can be expressed as

$$\cos(\Omega_C t_1) \sin^6[\pi J_{CH} \Delta] \cos(\pi J_{CC}(ct + 2\Delta)), \quad [a]$$

where  $\Omega_C$  is the carbon offset,  $J_{CH}$  and  $J_{CC}$  are the proton–carbon and carbon–carbon coupling constants, respectively. Since the signal intensity is not modulated by  $J_{CC}$  during the *t*<sub>1</sub> evolution time, the resulting HQQC spectrum will not contain splittings due to this coupling. In this simple con-

\* G.L.S., H.R.M., and I.D.C. thank the Wellcome Trust for financial support and the OCMS for the use of NMR and computing facilities. L.M. and H.O. acknowledge a grant from the BMBF.

§ Present address: Department of Biochemistry and Biophysics, University of North Carolina, Chapel Hill, North Carolina 27599.

|| To whom correspondence should be addressed.

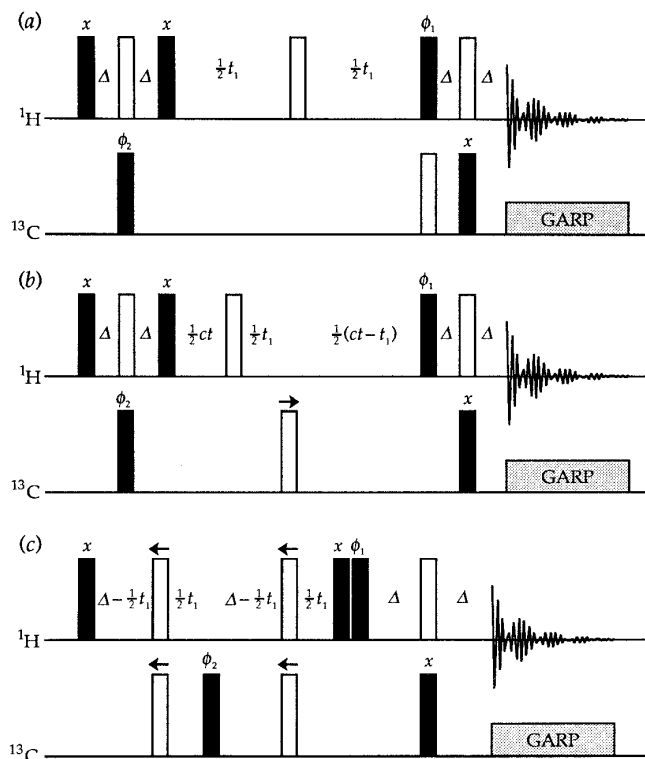


**FIG. 1.** Pulse sequences showing (a) the HQQC experiment, (b) the simple constant-time HQQC experiment, and (c) the new constant-time HQQC experiment respectively. Pulses with a nominal flip angle of  $90^\circ$  are shown in black,  $\pi$  pulses are shown in white. In the constant-time experiments, the arrows are used to indicate the direction in which the pulses are shifted as  $t_1$  is incremented; the  $\Delta$  delay was set to 4 ms. All unlabeled pulses were applied with phase  $x$ . The phase cycle used in these experiments was  $\phi_1 \{0, 60, 120, 180, 240, 300\}$ ,  $\phi_2 \{6(x), 6(-x)\}$ , and receiver  $\{2(0, 120, 240), 2(180, 300, 60)\}$ . Frequency discrimination in  $F_1$  was achieved by incrementing  $\phi_2$  in accordance with the States-TPPI procedure.

stant-time HQQC experiment, the proton-carbon couplings will not evolve during the constant-time period since the desired magnetization is present as heteronuclear quadruple-quantum coherence.

The simple HQQC experiment has two disadvantages: (i) the length of the experiment has been increased compared to the non-constant-time version causing a loss in sensitivity due to relaxation, and (ii) the intensity of the final signal has an inconvenient dependence on the length of the constant-time period. Assuming a carbon-carbon coupling of 35 Hz and ignoring relaxation, the signal intensity will be a minimum when  $ct = 6.3$  ms and a maximum when  $ct = 20.6$  ms. To obtain reasonable resolution,  $ct$  should be in the region of 8–12 ms which, unfortunately, falls fairly close to the intensity minimum. In practice, for our IL-2 sample, the best intensities were observed using a constant-time period in the range 13–14 ms. A constant-time period on this order means that large losses in sensitivity occur due to

relaxation, making the experiment rather insensitive. Figure 2 shows slices taken from an HQQC spectrum (2a, 2c) and a simple constant-time HQQC spectrum (2b, 2d), both recorded using a maximum value of  $t_1$ ,  $t_{1,\max}$ , of 14 ms. From these spectra, it is clear that the simple constant-time experiment does indeed provide higher resolution, but the loss in sensitivity is unacceptable.

An alternative method for monitoring the carbon offsets during a constant-time delay is to use the delays required for transferring magnetization from proton to carbon as constant-time evolution periods. An implementation of this idea is shown in Fig. 1c. In the new constant-time HQQC experiment, the second and third  $\Delta$  delays are used as a constant-time period in which the  $^{13}\text{C}$  offset is monitored. Both the first and the second pairs of  $180^\circ$  pulses must be shifted through the appropriate  $\Delta$  delays to enable the  $^{13}\text{C}$  offsets to be monitored while still refocusing the evolution of the proton chemical shifts. The signal intensity at the start of acquisition depends on

$$\cos(\Omega_{\text{C}}t_1) \sin^6(\pi J_{\text{CH}}\Delta) \cos(\pi J_{\text{CC}}2\Delta) \quad [b]$$

which shows that the signal intensity is not modulated by the carbon-carbon couplings during  $t_1$ . The new experiment should thus show better resolution than the non-constant-time version, and it should also be more sensitive since it is shorter when  $t_1 > 0$ .

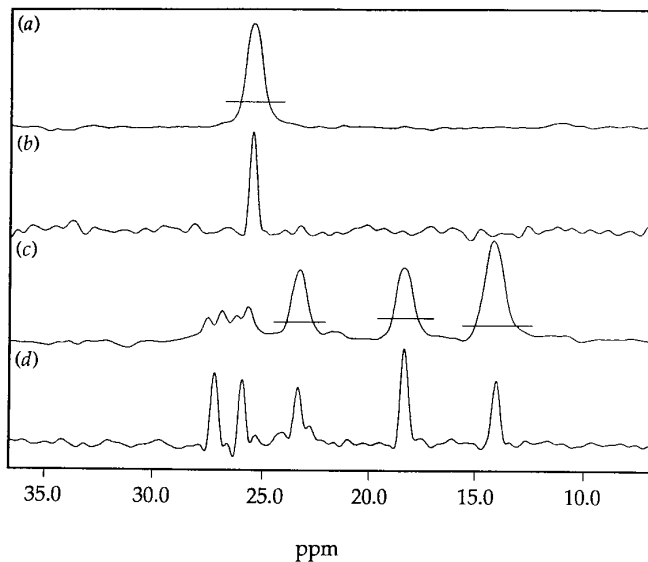


**FIG. 2.** Strips taken from HQQC spectra recorded on IL-2 using (a, c) the non-constant-time experiment and (b, d) the simple constant-time experiment. The higher resolution exhibited by traces (b, d) is readily apparent. The poor sensitivity of the simple constant-time experiment is illustrated by the lines marked on traces (a, c) which indicate the intensities of the corresponding peaks from the non-constant-time experiments shown in traces (b, d), respectively.

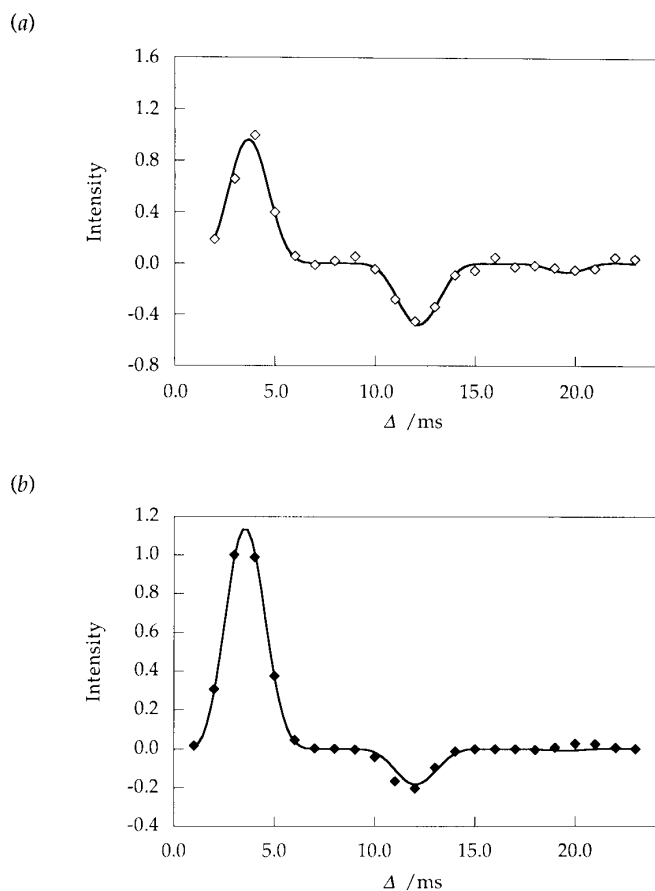


**FIG. 3.** Plots showing the signal intensity from a one-dimensional HMQC spectrum acquired using the new constant-time sequence with different values of the  $\Delta$  delay. (a) shows data acquired using the GFL peptide and (b) shows data acquired using a core residue of IL-2. The transfer function, Eq. [b], has been fitted to the data using  $J_{CC} = 35$  Hz and  $J_{CH} = 123$  Hz. For convenience, the relaxation behavior during the  $\Delta$  delay has been modeled using a single exponential decay with a fitted relaxation rate of 30 and 60 Hz for the GFL and IL-2 data, respectively. Although the loss of signal due to relaxation during the  $\Delta$  delays is expected to have a multiexponential form, the single-exponential form works well in practice.

The value of  $t_1$  in the new constant-time experiment is limited to  $2\Delta$  which somewhat restricts the choice of  $t_{1,\max}$  since the signal intensity depends strongly on the choice of  $\Delta$  as shown in Eq. [b]. Increasing  $\Delta$  with the aim of obtaining higher resolution results in dramatic losses in sensitivity. Intensities of peaks from one-dimensional HMQC spectra of the so-called GFL peptide sample, an eight-residue peptide with the sequence YGGFLRRI in which the segment GFL is uniformly labeled with  $^{15}\text{N}$  and  $^{13}\text{C}$ , and the IL-2 sample are shown in Fig. 3. These plots show that values of  $\Delta$  which differ from  $(2n - 1)/2J_{CH}$ , where  $n$  is an integer, result in large sensitivity losses. If the resolution requirements dictate that  $t_{1,\max}$  must be larger than 10 ms then, to obtain optimal sensitivity,  $\Delta$  should be set about 12 ms,

allowing for the use of any value of  $t_{1,\max}$  up to 24 ms. Figure 4 shows HMQC spectra of IL-2 acquired using the new constant-time sequence with  $\Delta$  set to 4, 5, and 12 ms. The spectrum recorded with  $\Delta$  set to 12 ms shows significant losses in sensitivity for the less mobile residues, although at a sufficiently low contour level all cross peaks are visible. This suggests that spectra recorded using long values of  $\Delta$  will generally only be useful for small proteins or concentrated samples of larger proteins. It should be noted, however, that the sensitivity of the new constant-time experiment with  $\Delta$  set to 12 ms is higher than the sensitivity of the simple constant-time experiment for all values of  $ct$  between 8 and 20 ms; clearly, the new experiment is the better method for recording constant-time HMQC spectra.

The improvement in resolution obtained using the new constant-time experiment can be seen in Fig. 5. This figure shows cross sections taken from HMQC spectra recorded using both the old HMQC sequence, lower traces, and the new constant-time HMQC sequence, upper traces, on a sample of the GFL peptide. Figure 5a displays cross sections from spectra recorded using a value of  $t_{1,\max}$  of 8 ms. The improved resolution and sensitivity is evident from these spectra. Figure 5b contains the same cross sections taken from spectra processed with  $t_{1,\max}$  extended to 16 ms (for the old experiment, this was achieved by increasing the acquisition time in  $t_1$  and for the new constant-time experiment by using mirror-image linear prediction). The improvement in resolution for the new experiment is even more evident from these traces.

The improved resolution of the new constant-time HMQC spectrum is also illustrated using spectra of IL-2 in Fig. 6. The HMQC spectrum acquired using the old sequence is shown in Fig. 6a and the spectrum acquired using the new sequence is shown in Fig. 6b. Both spectra have been processed using a value of  $t_{1,\max}$  of 16 ms and have been plotted at the same level. Although contour plots do not give a quantitatively accurate picture of resolution, it is quite clear from this diagram that the new constant-time experiment provides significantly better resolution than the old experiment. The resolution in the new constant-time experiment is certainly sufficient to resolve most of the methyl–methyl NOEs for this protein using a constant-time HMQC–NOESY experiment.

The HMQC experiment manipulates magnetization which originates on the methyl protons, making it possible to suppress the water signal using presaturation without sustaining unacceptable losses in sensitivity. Although the methyl proton signals are well separated from the water resonance, presaturation can still reduce the sensitivity of the HMQC experiments as a result of spin diffusion from protons with similar chemical shifts to the water (13). An alternative method of water suppression is to use a gradient-selective pulse combination, such as Watergate or the double-gradi-

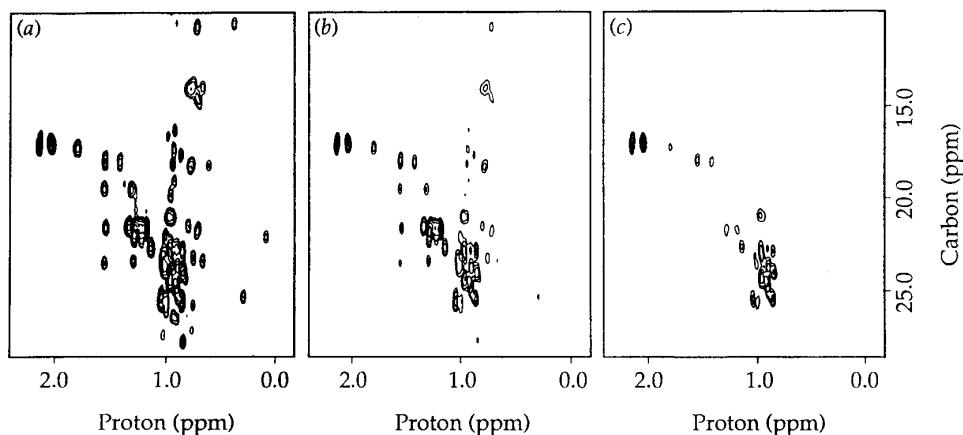


**FIG. 4.** HMQC spectra of IL-2 recorded using the new constant-time HMQC sequence with  $\Delta$  set to (a) 4, (b) 5, and (c) 12 ms. All spectra have been acquired using a value of  $t_{1,\max}$  of 8 ms and have been processed identically. The loss in sensitivity associated with increasing  $\Delta$  is apparent; however, it should be noted that at a lower contour level in spectrum (c) all cross peaks are visible.

ent-echo method, to dephase the water signal (14, 15). The HMQC spectrum of IL-2 showed a loss in sensitivity of approximately 20% when presaturation was used for water suppression. There was no noticeable improvement in sensitivity when the gradient-selective-pulse methods were used for water suppression. Although these methods do not saturate the alpha protons during the recycle delay, they do lengthen the experiment, and hence sensitivity losses can result from relaxation during the time required for the gradient and selective pulses. Consequently, we chose to use presaturation for water suppression because it is easier to implement.

The new constant-time HMQC pulse sequence is quite sensitive to imperfections in the  $^{13}\text{C}$   $180^\circ$  pulses. Such imperfections can introduce unwanted signals into the HMQC spectrum, which may need to be suppressed (16, 17). If the carbon pulses have been calibrated correctly and if the carbon transmitter is placed in the methyl region of the spectrum, these unwanted signals should be small. They can, however, be removed completely by adding a pair of weak gradient pulses around both the carbon  $180^\circ$  pulses in the constant-time evolution periods. The addition of gradient pulses in the constant-time period will have the effect of reducing slightly the achievable resolution, if  $\Delta$  is unaltered,

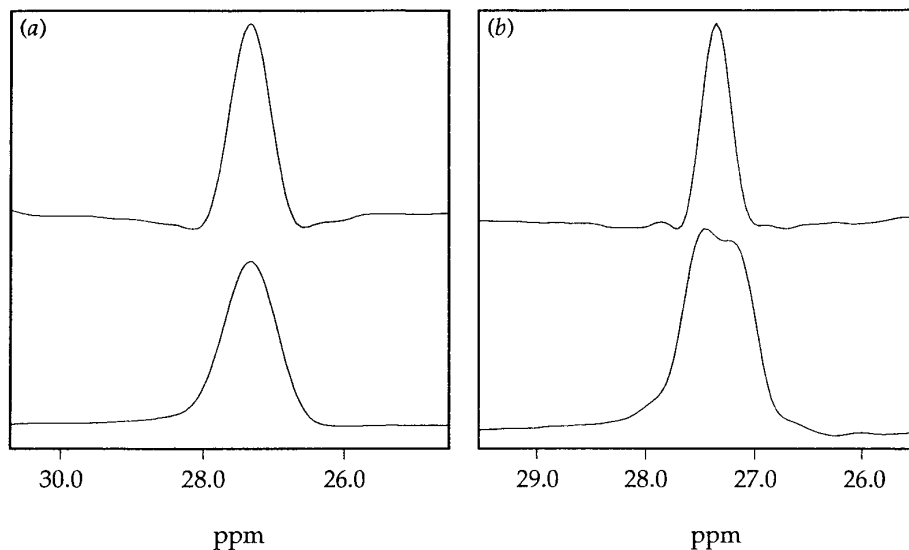


**FIG. 5.** Slices taken from an HMQC spectrum acquired using the old pulse sequence, lower trace, and the new HMQC pulse sequence, upper trace, using the GFL peptide sample. (a) shows the data acquired with a  $t_{1,\max}$  of 8 ms, while (b) shows the data acquired using a  $t_{1,\max}$  of 16 ms, lower trace, and data extended to a  $t_{1,\max}$  of 16 ms using mirror image linear prediction, upper trace. The higher resolution and sensitivity of the new experiment is apparent from (a). The improvement in the resolution of the new experiment is more marked in (b) where the limiting resolution has been increased.

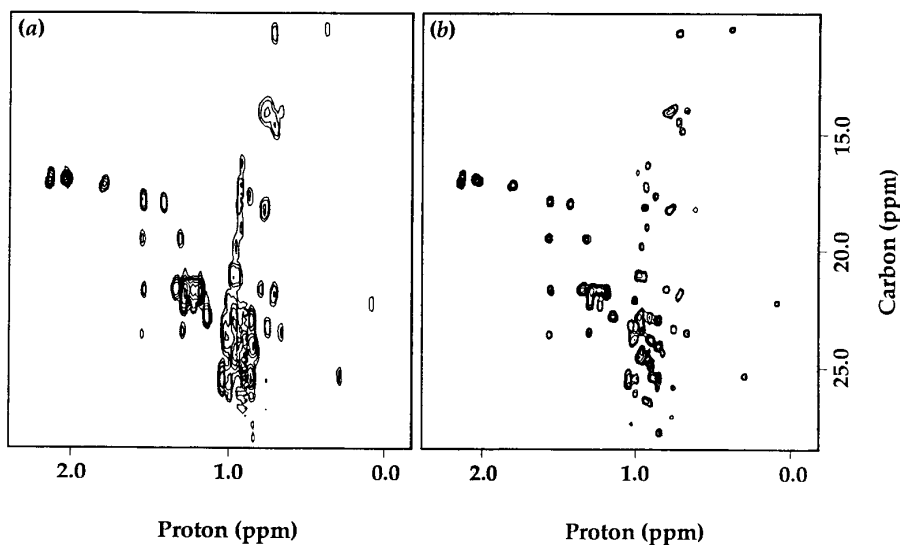


**FIG. 6.** HMQC spectra of IL-2 acquired using (a) the old HMQC pulse sequence and (b) the new constant-time HMQC pulse sequence. Both spectra use a  $t_{1,\max}$  of 16 ms which has been achieved in (b) by using mirror image linear prediction and in (a) by acquiring additional points in  $t_1$ .

or reducing slightly the sensitivity if  $\Delta$  is increased to allow for the time required for the gradient pulses. If short (60  $\mu$ s) gradient pulses are used, the losses in sensitivity or achievable resolution are small.

Data were collected using homebuilt spectrometers operating at  $^1\text{H}$  frequencies of 600 and 750 MHz, at a temperature of 30°C. The sample of the IL-2 mutant was dissolved in 450  $\mu$ l  $\text{H}_2\text{O}$  and 50  $\mu$ l of  $\text{D}_2\text{O}$ . The GFL peptide was obtained from Cambridge Isotopes dissolved in  $\text{DMSO-}d_6$ . When presaturation was used for water suppression, a 104 Hz RF field was applied at the water frequency during the recycle delay. The field strengths used for the high power  $^1\text{H}$  and  $^{13}\text{C}$  pulses were 20 and 12.8 kHz, respectively. Decoupling of  $^{13}\text{C}$  was achieved using the GARP sequence (18) with a decoupling field strength of 2.5 kHz. The proton transmitter was shifted from the water resonance, after presaturation, to the middle of the methyl-proton region (1.08 ppm); the carbon transmitter was positioned at 20.3 ppm. The HMQC spectra of the GFL peptide were acquired at 600 MHz using spectral widths of 7500 and 10,000 Hz in  $F_1$  and  $F_2$ , respectively. The  $^{13}\text{C}$  transmitter was positioned at 26.3 ppm in these spectra. The HMQC spectra of IL-2 were acquired at 750 MHz using spectral widths of 4149 and 12,500 Hz in  $F_1$  and  $F_2$ , respectively; the  $^{13}\text{C}$  transmitter was positioned at 20.3 ppm. Data were processed using a mild Gaussian window function in  $F_2$  and a Kaiser apodization function in  $F_1$ .

## REFERENCES

1. K. Wüthrich, "NMR of Proteins and Nucleic Acids," Wiley, New York, 1986.
2. C. Redfield, L. J. Smith, J. Boyd, G. M. P. Lawrence, R. G. Edwards, R. A. G. Smith, and C. M. Dobson, *Biochemistry* **30**, 11,029 (1991).
3. S. W. Fesik and E. R. Zuiderweg, *J. Magn. Reson.* **78**, 588 (1988).
4. D. Marion, L. E. Kay, S. W. Sparks, D. A. Torchia, and A. Bax, *J. Am. Chem. Soc.* **111**, 450 (1989).
5. H. R. Mott and I. D. Campbell, *Curr. Opin. Struc. Biol.* **5**, 114 (1995).
6. H. R. Mott, B. S. Baines, R. M. Hall, R. M. Cooke, P. C. Driscoll, M. P. Weir, and I. D. Campbell, *J. Mol. Biol.* **247**, 979 (1995).
7. H. Kessler, P. Schmieder, and H. Oschkinat, *J. Am. Chem. Soc.* **112**, 8599 (1990).
8. J. M. Schmidt and H. Rüterjans, *J. Am. Chem. Soc.* **112**, 1279 (1990).
9. H. Kessler, P. Schmieder, M. Köck, and M. Reggelin, *J. Magn. Reson.* **91**, 375 (1990).
10. D. M. Doddrell, D. T. Pegg, and M. R. Bendell, *J. Magn. Reson.* **48**, 323 (1982).
11. A. Bax, A. F. Mehlkopf, and J. Smidt, *J. Magn. Reson.* **35**, 167 (1979).
12. M. G. Munowitz, R. G. Griffin, G. Bodenhausen, and T. H. Huang, *J. Am. Chem. Soc.* **103**, 2529 (1981).
13. S. H. Smallcombe, *J. Am. Chem. Soc.* **115**, 4776 (1993).
14. M. Piotto, V. Saudek, and V. Sklenář, *J. Biomol. NMR* **2**, 661 (1992).
15. T. Hwang and A. J. Shaka, *J. Magn. Reson. A* **112**, 275 (1995).
16. A. Bax and S. S. Pochapsky, *J. Magn. Reson.* **99**, 638 (1992).
17. G. L. Shaw and J. Stonehouse, *J. Magn. Reson. B* **110**, 91 (1996).
18. A. J. Shaka, P. B. Barker, and R. Freeman, *J. Magn. Reson.* **64**, 547 (1985).